2023

AGE AND CHEMISTRY OF BELL CREEK BATHOLITH

Elana G. Barth
Michigan Technological University, egbarth@mtu.edu

AGE AND CHEMISTRY OF BELL CREEK BATHOLITH

By

Elana G. Barth

A REPORT

Submitted in partial fulfillment of the requirements for the degree of

MASTER OF SCIENCE

In Geology

MICHIGAN TECHNOLOGICAL UNIVERSITY

2023

This thesis has been approved in partial fulfillment of the requirements for the Degree of MASTER OF SCIENCE in Geology.

Department of Geological and Mining Engineering and Sciences

Thesis Advisor:	*Dr. Chad Deering*
Committee Member:	*Dr. Jeremy Shannon*
Committee Member:	*Dr. Jim DeGraff*
Department Chair:	*Dr. Aleksey Smirnov*

Table of Contents

List of Figures

List of Tables

Author Contribution Statement

Anna Dalle Fratte and Brandi Petry for their geochemical and U-Pb zircon datasets.

Acknowledgements

Thank you to Dr. Chad Deering for his support and guidance. I would also like to thank Emmeline Wolowiec for taking my samples to Zurich and getting the raw zircon data for me. Furthermore, thanks to The Department of Geological and Mining Engineering and Sciences at Michigan Tech for all of the opportunities and support over the last six years. Lastly to my family and friends for your love and encouragement.

Abstract

The Southern Complex, located near Marquette, Michigan is in the southernmost portion of the Superior Province. This complex consists of granitoids and granitic gneiss that vary in composition. In twentieth century research, Hoffman (1987) and Tinkham (1997) concluded that the Southern Complex contained two units in which the granitoid was emplaced in the granitic gneiss. Recent research conducted by Petryk (2019) determined that the Southern Complex has a U-Pb zircon age of 2600 Ma. Dalle Fratte (2020) concluded that the granitic gneiss migmatite texture was the result of a felsic magma mixing with several generations of mafic intrusions that were later deformed. Data from Petryk (2019) and Dalle Fratte (2020) were mostly from M-95, which only accounts for the western portion of the Southern Complex.

More geochemical and isotope data were collected from the eastern portion of the Southern Complex and compared with previous studies. The U-Pb zircon ages from the eastern portion of the Southern Complex were approximately 2600 Ma, similar to data from Petryk (2019) and Tinkham (1997). The eastern side also yielded some data with slight variations in geochemistry, which supports Dalle Fratte (2020) interpretation; magma mixing between a felsic melt and several generations of a more mafic melt intruding the pluton during or later in its crystallization.

1 Introduction

Archean cratons only make up seven percent of the Earth's crust yet these limited exposures provide unique access to study Archean tectonics, crust-mantle petrogenesis, and crustal growth. The Canadian Shield is the world's largest relatively undisturbed craton and includes the Superior Province (Card,1986). The Southern Complex found near Marquette, Michigan represents the southernmost portion of the Superior Province (Figure 1).

This complex consists of granitoids and granitic gneiss that vary in composition. The Southern Complex is broken into two broad categories: 1) granitoids and 2) deformed granitoids; however, these groups vary widely in composition and texture. The ages of the groups vary but the granitoid gneiss is interpreted to be older than the granitoid, though both groups fall within the Late Archean. The limited amount of previous work on the Southern Complex has led to inconclusive and sometimes contradictory models regarding their formation.

Historically, two studies focused on the Southern Complex. The first, by Hoffman (1987), focused on geochemistry and textural variability to determine the formation. This study concluded the Bell Creek Granite was an S-type granite that was emplaced into a deformed metasediment or metavolcanic suite of basement rocks. The second, by Tinkham (1997), focused on structural aspects related to the tectonic evolution and included the first radiometric dating of the formation. This study concluded there were two units within the Southern Complex and that the granitic gneiss was likely older than the granitoid.

In contrast to the previous studies, Petryk (2019) used an extensive geochronological and geochemical database and determined that the granitoids evolved by a process of crystal fractionation from mantle-derived magma that included recycling of supracrustal material. Importantly, this indicates a period of crustal growth during the Archean. A companion study by Dalle Fratte (2020) concluded that the deformed outcrops previously interpreted to be migmatitic in origin were more likely igneous in origin. Detailed textural analysis indicated that the mafic-felsic relationship was instead the result of a felsic magma mixing with several generations of mafic intrusions that were later deformed.

The recent studies focused on the western side of the complex; however, the Southern Complex extends to the east tens of kilometers. The objective of this study was to obtain a complementary dataset to that of Petryk (2019) including bulk-rock geochemistry and zircon U-Pb dating.

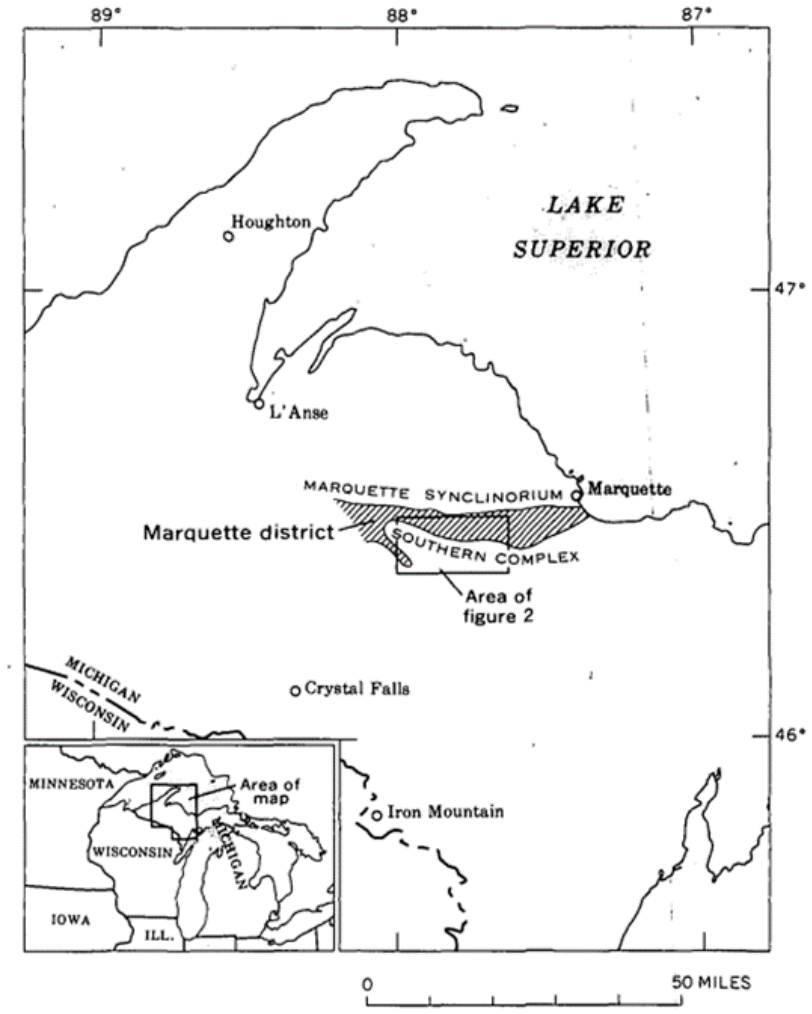

Figure 1. The Southern Complex within the Upper Peninsula with reference to the Marquette Syncline (shaded area) (Cannon and Simmons, 1973). The inlay in the lower left corner shows the location of the study area within Michigan.

2 Geologic Background

Hoffman and Tinkham both divided the Southern Complex into two units, one granitoid and one a deformed granitoid. The Bell Creek Granitoid varies in texture, including fine-grained, coarse-grained and porphyritic rock types. Mineralogically the Bell Creek Granitoid is comprised mostly of K-feldspar megacrysts with lesser amounts of quartz, plagioclase, and biotite. The Bell Creek Gneiss is similar to the Bell Creek Granitoid in mineralogy but displays a strong foliation.

Hoffman (1979) was the first to define a subgroup within the Bell Creek Granitoid, The Bell Creek Clotted Granitoid as dark ovoid splotches or clots of mafic minerals contained in a matrix of coarse-grained to pegmatitic leucogranite. Clots are composed of biotite, chlorite, garnet, quartz, and feldspar. Hoffman defined the groups based on textural variability, not chemical variability. Bulk-rock chemistry indicated that the Southern Complex is a peraluminous, corundum-normative granitoid. However, when compared to "normal" granitoids as defined by Krauskopf (1967) and Barth (1952). Hoffman (1979) found the Bell Creek Granite to be high in potassium, uranium, and thorium but low in calcium, ferrous iron, and strontium.

Calculated ages of the different units within the Southern Complex differ between studies. Van Schmus and Woolsey (1975) used Rb/Sr whole rock values to calculate a model age of the Southern Complex that placed it within the Late Archean. Hammond (1978) used U-Pb zircon dating, which provides a more precise age for the Compeau Creek Gneiss (2779±21 Ma). Tinkham (1997) used zircon U-Pb dating to calculate the age of the granitoid was determined to be 2613.6 +4.1/-3.7 Ma, but only three ages were used to calculate this Discordia upper intercept age. The deformed granitoid had two

calculated ages, one which was 2703 Ma and one 3093 Ma. Both ages are slightly older than the undeformed granitoid, so Tinkham (1997) interpreted that the deformed unit was different and older than the undeformed unit, with the deformed unit being at least 3100 Ma (Figure 2). Petryk (2019) calculated zircon U-Pb ages from 13 granitoids to be 2.55±0.048 Ga. Petryk's interpretation differed from Tinkham's where older grains were not interpreted to be an older unit, but instead inherited grains from assimilation of country rock.

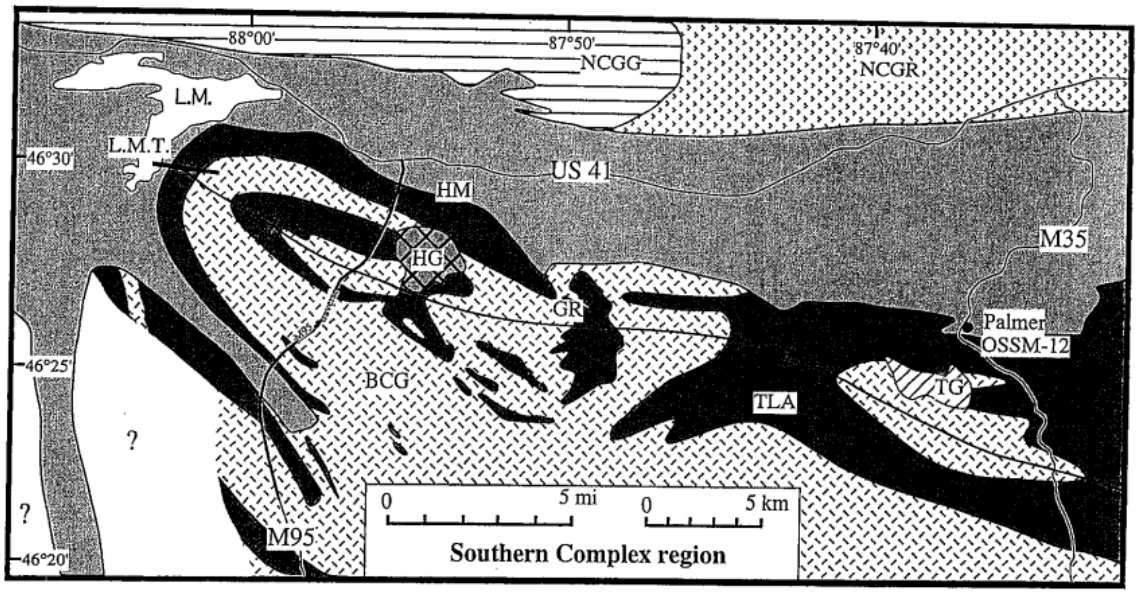

Figure 2. Geologic map of the Southern Complex. LM= Lake Michigamme, NCGR=Northern Complex greenstone terrane, NCGG= granitoid, and gneiss of the Northern Complex, BCG= Bell Creek Granitoid and Gneiss, TLA= Twin Lake Assemblage, TG= Tilden Granitoid, HG= Humboldt Granitoid, L.M.T.= Lake Michigame Transverse, HM= Humboldt Mine, GR= Greenwood Reservoir. M95 traverse is along a thickened portion of the M95 line. Tinkham (1997) modified from Hoffman (1987).

Hoffman (1979) concluded that the Bell Creek Granitoid is an S-type granitoid derived from partial melting of graywacke or arkose, with some minor compositional variation due to crystal fractionation. The Bell Creek Granitoid was emplaced into the deformed unit during a period of regional deformation that produced double plunging folds (Hoffman, 1979). Tinkham (1997) interpreted that the granitoid intruded and folded

the deformed granitoid, which was originally a dome. He also suggested that the deformed granitoid could be a part of a granitic-greenstone terrane like the Wawa Sub-province of the Superior Province, Canada.

Based on oxygen and hafnium isotopes in zircons, Petryk (2019) concluded that the Southern Complex was produced by crystal fractionation from a primary, mantle-derived magma, rather than through partial melting of a crustal basement. Petryk did show that there was some amount of recycling of a pelitic supracrustal source during emplacement at about 2.6 Ga. Zircon U-Pb dating included inherited grains in the granitoids up to 4.2 Ga, which were likely derived from assimilation of the pre-existing crustal rocks of the Superior Province. Petryk's U-Pb zircon dates also showed that the Clotted Granitoids described by Hoffman are not a separate unit and are instead the same as the Bell Creek Granitoids and the clots are likely preserved remnants of assimilation of the pelitic material (clots include chlorite, garnet, and biotite). Dalle Fratte (2020) found the doming structure of the batholith was formed before it was exhumed, but magma from the felsic melt of the batholith mixed with several generations of more mafic magma while both components were liquid.

3 Methods

3.1 U-Pb zircon dating

Eleven samples collected from the field in 2019 (Figure 3) were processed to extract zircons using standard techniques by Zirchron (Appendix 1). The zircons were mounted at Michigan Tech and subsequently set in epoxy and polished by Wagner Petrographic. Backscatter electron images were collected from the Michigan Tech ACMAL lab using a Philips XL 40 ESEM. The zircons were covered in 7 nm platinum-palladium coating with carbon tape. The backscattered-electron images and secondary electron images of the zircon were examined to identify zones appropriate for U-Pb dating and trace element analysis. The samples were analyzed at Eidgenössische Technische Hochschule (ETH) Zürich using a Resonetics Resolution S155 laser ablation system coupled to a Thermo Element XR Sector-field ICP-MS with a 20μm beam diameter.

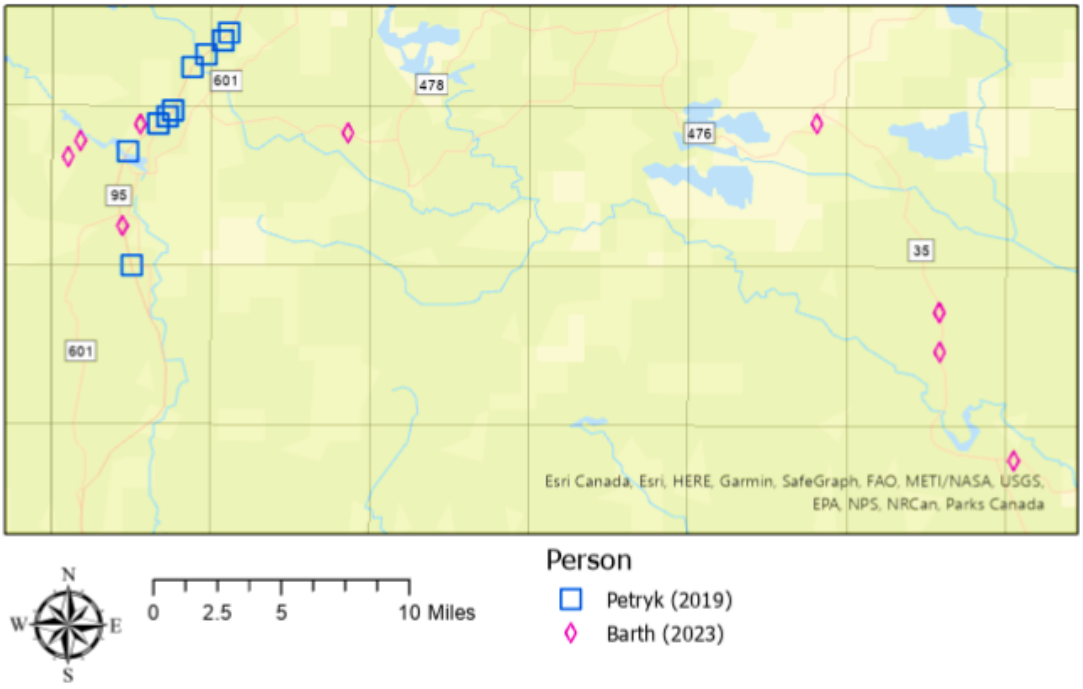

Figure 3: Location map for samples with extracted zircons. Blue squares indicate data from Petryk (2019) and pink diamonds indicate samples from this paper. Orange lines indicate roads, most samples are from M-95 to the west or M-35 to the east.

The data were then processed using Iolite4™. Each zircon was selected manually, due to the algorithm tending to be less accurate with older samples. The data were selected by displaying the Beam Series: ^{27}AL_CPS, ^{204}Pb_CPS, ^{31}P_CPS, ^{91}Zr_CPS, ^{238}U_CPS, ^{139}La_CPS, Final ^{207}Pb/^{206}Pbage, Final ^{207}Pb/^{235}U age, Final U/Th, Final^{206}Pb/^{238}Uage. Plateau represents areas with no inclusions within the grain and was selected for data analysis. Trends of spikes in the elements indicate the laser hitting something other than lead or uranium in the sample, due to contamination within the grain and these areas were excluded from subsequent analysis. Data reduction schemes for Uranium-Lead were calculated GJ1 as a reference. Stacy-Krammers Lead correction was then applied to the data (Petrus, J.A. and Kamber, B.S., 2012). Exported data

includes the mean, 2SE, mean age, mean age 2SE, and correlation(rho) for the ratios: $^{206}Pb/^{238}U$, $^{238}U/^{206}Pb$, $^{207}Pb/^{206}Pb$, $^{208}Pb/^{232}Th$ (Appendix 2).

The data calculated from Iolite4 was processed using IsoplotR (Vermeesch, 2018). $^{238}U/^{206}Pb$ and $^{207}Pb/^{206}Pb$ within error of 2SE were used to calculate Wetherill Concordia and Discordia (Model 1) ages including propagated external uncertainty (Figure 4). Data with errors greater than one standard deviation were omitted from the dataset to reduce the uncertainty of the discordia and MSWD (Mean Square of the Weighted Deviation) errors (Appendix 3).

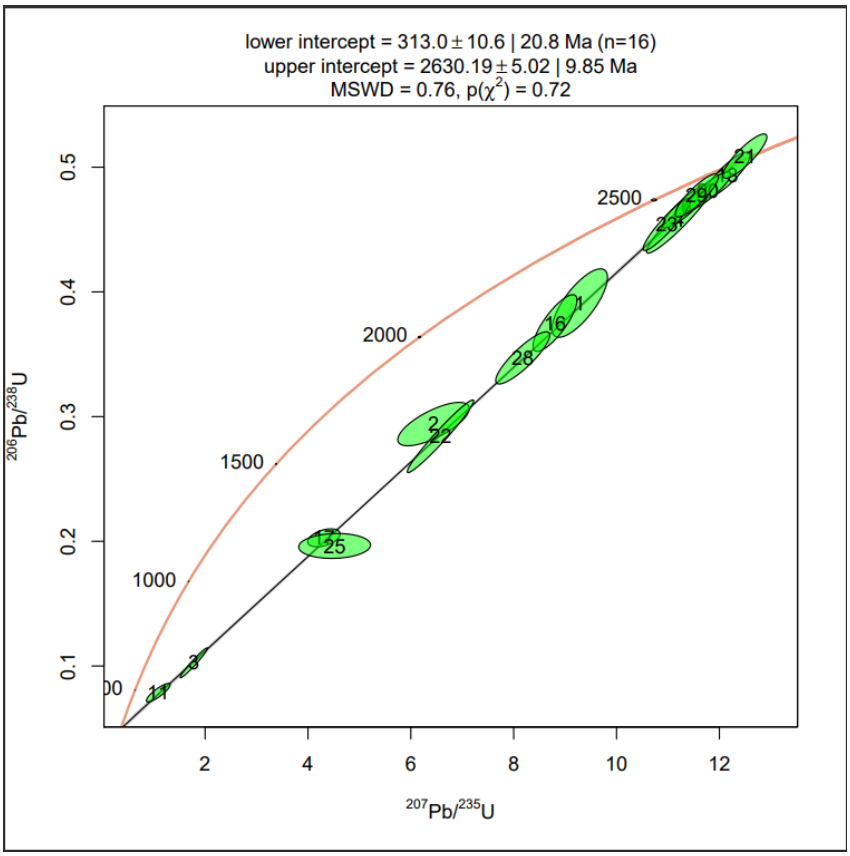

Figure 4. Example of a Concordia plot for sample MQ-120. Red line indicates the Concordia measured in Ma, black line represents the Discordia. The green ovals represent the error for the calculated age.

The $^{238}U/^{206}Pb$ and $^{207}Pb/^{206}Pb$ values with an error of 2SE were used to calculate $^{207}Pb/^{206}Pb$ ages (Appendix 4). There was no common Pb correction (Stacey-Krammers)

because it was applied in Iolite4, so the measured values had already been corrected for common lead. Outliers were omitted from the calculation for a more precise age. Not all MSWD values are below one, though all are below ten. This was done for samples with fewer crystallization ages to reduce any artificial inflation in the mean $^{207}Pb/^{206}Pb$ ages for each sample.

Concordance percent is the percent difference between two of the three ages calculated in IsoplotR. Most of the dates are older than one Ga so the difference between $^{207}Pb/^{206}Pb$ and $^{206}Pb/^{238}U$ is because $^{206}Pb/^{207}Pb$ have more accurate ages for older zircons. A few metamorphic grains have an age below one Ga, the concordance percent for these was calculated using $^{207}Pb/^{235}U$ and $^{206}Pb/^{238}U$ because $^{207}Pb/^{235}U$ has a more accurate age for younger zircons. Ages with concordance below 85 percent and above 105 percent were not considered in the analysis.

3.2 Bulk-rock Chemistry

Bulk-rock compositions of 30 samples were determined by Activation Laboratories Ltd. Rock samples were first crushed and mixed with a flux of lithium metaborate and lithium tetraborate and fused in an induction furnace. The major and trace elements were obtained using a Perkin Elmer Sciez ELAN 6000 inductively coupled mass spectrometry (ICP-MS). Three blanks and five control samples were analyzed with each group of unknown samples and the instrument was recalibrated every 40 samples (Appendix 5).

4 Results

4.1 U-Pb Zircon Ages

Concordia ages were calculated to determine the crystallization and/or metamorphic age for domains within each zircon (Table 1). Concordia ages are determined by calculating where the Discordia intersects the Concordia. The upper Concordia value represents the approximate age of crystallization, with the majority of this data set approximately 2600 Ma, but ages can be slightly skewed by inherited and metamorphic grains (Appendix 6). The lower Concordia value represents the approximate age of the last metamorphic event, with all ages younger than 350 Ma.

Table 1. Summary table of the calculated ages for 11 samples from the Southern Complex.

Sample	U-Pb Mean Age (Ma)	Concordia Upper (Ma)	Concordia Lower (Ma)
MQ-116A	2587±13	2607.10±9.64	259.00±5.99
MQ-118	2602.1±4.6	2599.88±3.30	253.8±12.4
MQ-120	2620.5±5.5	2630.19±5.02	313.0±10.6
MQ-122	1349±13	1538.3±16.4	190.95±4.54
MQ-125	2587.0±8.8	2640.49±7.37	236.29±8.25
MQ-126B	2634.9±7.2	2632.85±7.96	187.37±4.61
MQ-130A	2548.0±6.9	2624.20±7.99	270.21±7.13
MQ-130C	2819.1±5.9	2694.37±9.48	201.64±3.24
MQ-160	2748.7±6.9	2492.6±17.7	170.02±3.50
MQ-109A	2458±22	2633.6±24.1	291.0±21.2
MQ-144	2548.5±6.7	2621.05±9.08	221.42±2.70

The spatial distribution of crystallization ages (including those of Petryk, 2019) was examined to determine if there are any patterns in ages between different rock types

and textures (Figure 5). However, there was no spatial correlation found across the study area related to the different rock types (i.e. migmatite, gneiss, granitoid) or textures (i.e. mixing or clots of assimilated material).

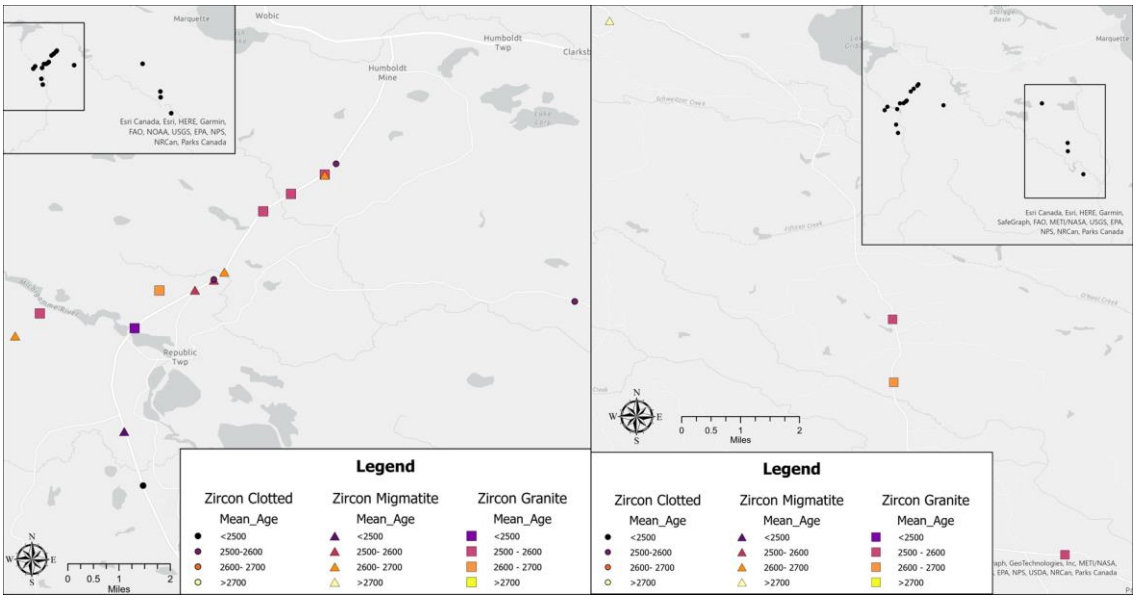

Figure 5. Mean U-Pb Age spatial distribution. Ages were divided into four manual breaks (100 million years per break). Shapes represent the texture of the sample: circles represent clotted granitoid, triangles represent migmatite zones, and squares represent the Bell Creek Granitoid.

4.2 Geochemistry

Bulk-rock chemistry for new samples was compared to data from Petryk (2019) and Dalle Fratte (2020). Bulk-rock chemistry for new felsic samples (N=33) was combined with felsic geochemical data from Petryk (2019, N=13) and from Dalle Fratte (2020, N=4) for a total sample count of 50.

4.2.1 Major Elements

The major element compositions of rocks from the studies of Petryk (2019) and Dalle Fratte (2020) are similar to those analyzed in this study. In particular, the granitoids, gneiss, and magmatic mixing are I-type, medium- to high-K_2O, and slightly

peraluminous. Below is a summary the variations in individual major elements of note (Figure 6).

Aluminum plotted in Figure 6 shows both Petryk (2019) and Dalle Fratte (2020) with linear trends, though the slopes are different. The new data partially fill a gap along a trend of decreasing Al_2O_3 with SiO_2 with a few outliers of higher Al_2O_3. Calcium (Figure 6) indicates no trend exists with the data of Dalle Fratte (2020), though it does fit within the two linear trends exhibited by Petryk (2019). Data from this study fills in the linear trend with the steeper slope from Petryk (2019) and is clustered around the smaller weight percent values from previous research. Petryk (2019) did have one outlier around 80 weight percent silica, and the additional data from this research did not support any trends including that outlier. Magnesium (Figure 6) is mostly clustered under one weight percent, however, Petryk (2019) and Dalle Fratte (2020) do have a few outliers with higher values. Roughly half of the data from this study have higher Na_2O at a given SiO_2 value than those from the previous work (Figure 6). Those same samples with higher Na_2O as seen in Figure 6 have lower K_2O than those from the previous studies (Figure 6). Therefore, although the Na_2O and K_2O differ in some of these units the 'total' alkalis are still very similar. Titanium values (Figure 6) are clustered below 0.4, except for one outlier from Petryk (2019). Phosphorous (Figure 6) are clustered below 0.1 weight percent, except for one outlier from Petryk (2019).

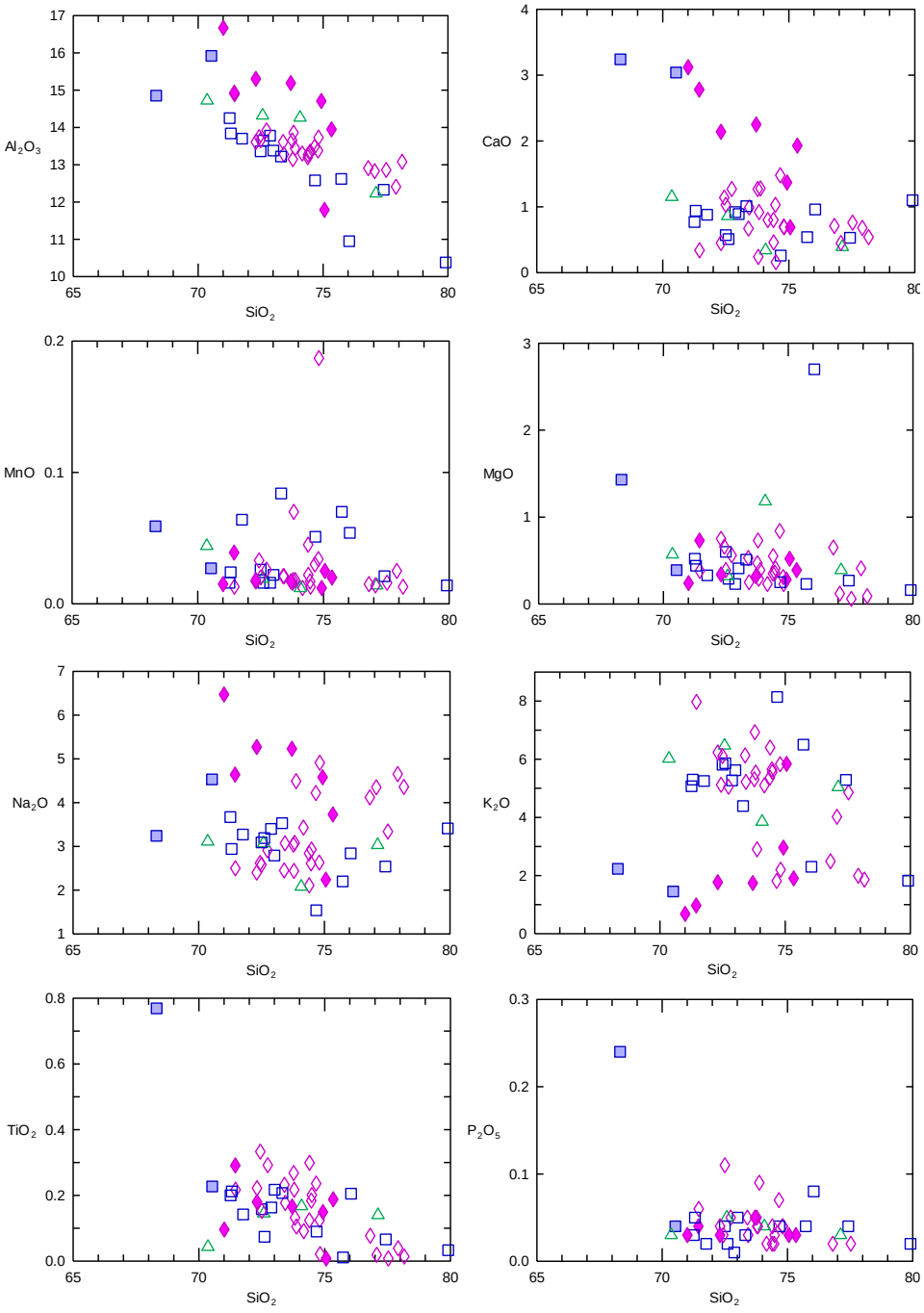

Figure 6. Bulk rock chemistry individual Harker Diagrams with major elements (weight percent) plotted against silica (weight percent). Green triangles represent data from Dalle Fratte (2020), blue squares represent from Petryk (2019), and pink diamonds represent data from this paper. Filled symbols represent high Ca or low K_2O.

4.2.2 Trace Elements

Trace element concentrations vary more than major element concentrations and, consequently, can provide more information about the source and subsequent processes that formed the rocks. Figure 7 displays the rare-earth elements (REE) normalized to chondrites. Data from all three data sets have similar trends, including negative and positive europium anomalies.

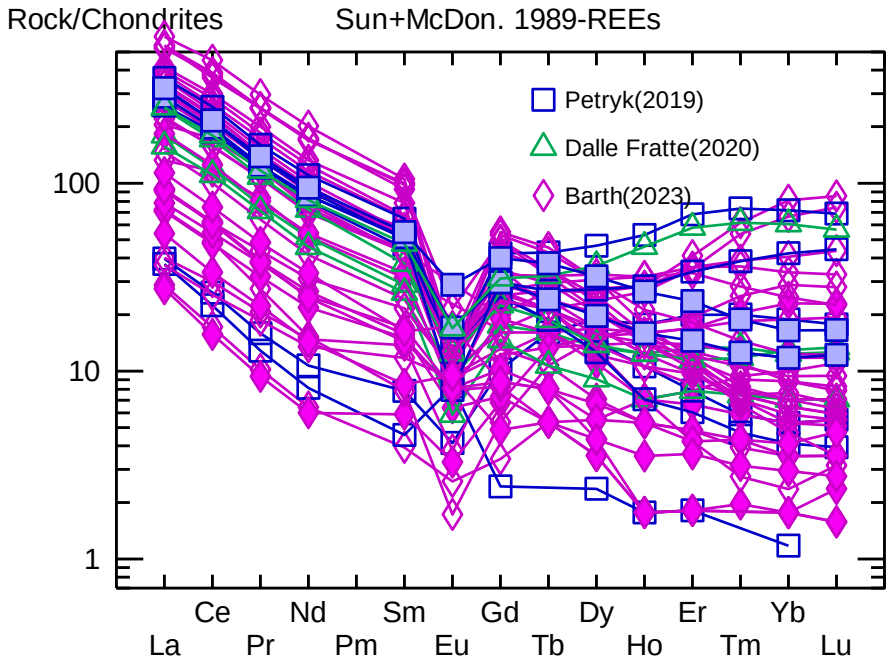

Figure 7. Bulk-rock REE normalized to chondrite.

REEs can also be normalized against a primitive mantle as shown in Figure 8. The heavy REE do not vary in any of the datasets unlike the light REE. Rubidium, thorium, uranium, and lead differ from the primitive mantle in all three datasets. Tantalum has two outliers which are relatively high (samples MQ-122 and MQ-123).

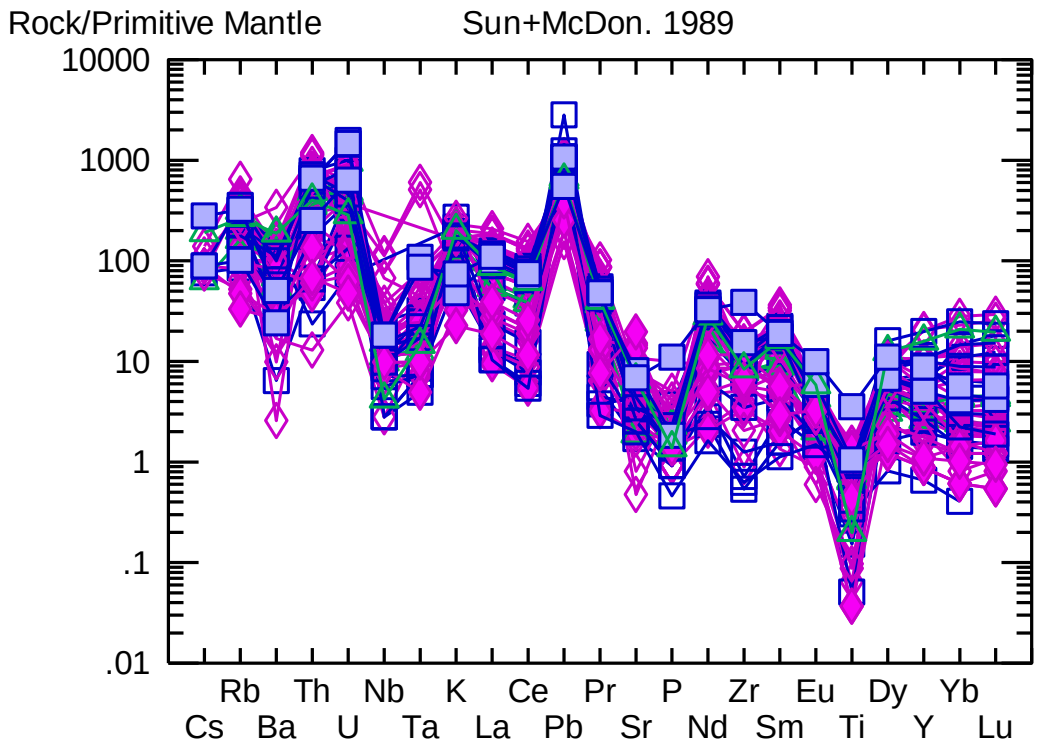

Figure 8. REEs normalized against primitive mantle. HREEs tend to have similar trends whereas the LREEs have more variance. However, all three data sets show the variance.

Bivariant plots of trace elements were plotted to illustrate variance in more detail. Figure 9 displays barium against lanthanum. Barium is an incompatible trace cation and lanthanum is the most incompatible REE. Most of the data is clustered between 1000 ppm of barium and 100 ppm with a few exceptions, the most notable being MQ-134 near the upper right corner if the figure. Strontium is incompatible in hydrothermal conditions whereas Rubidium is compatible (Figure 9).

There are five samples with relatively high strontium (MQ-130a, MQ-132c, MQ-132d, MQ-135c, and MQ-136). Niobium is clustered below 20 ppm (Figure 9), with four outliers with higher values (MQ-109a, MQ- 112a, MQ- 122, and MQ- 123). There are only four outliers for Yttrium including MQ-122, MQ-123 from this study, M95-ADF-046B Dalle Fratte (2020), and BCG-8A from Petryk (2019). For all the data lead is

clustered below 100 ppm and zirconium is clustered under 200 ppm, except for one outlier from Petryk (2019) (BCG-12b). No other trends can be determined from the lead and zirconium plot (Figure 9).

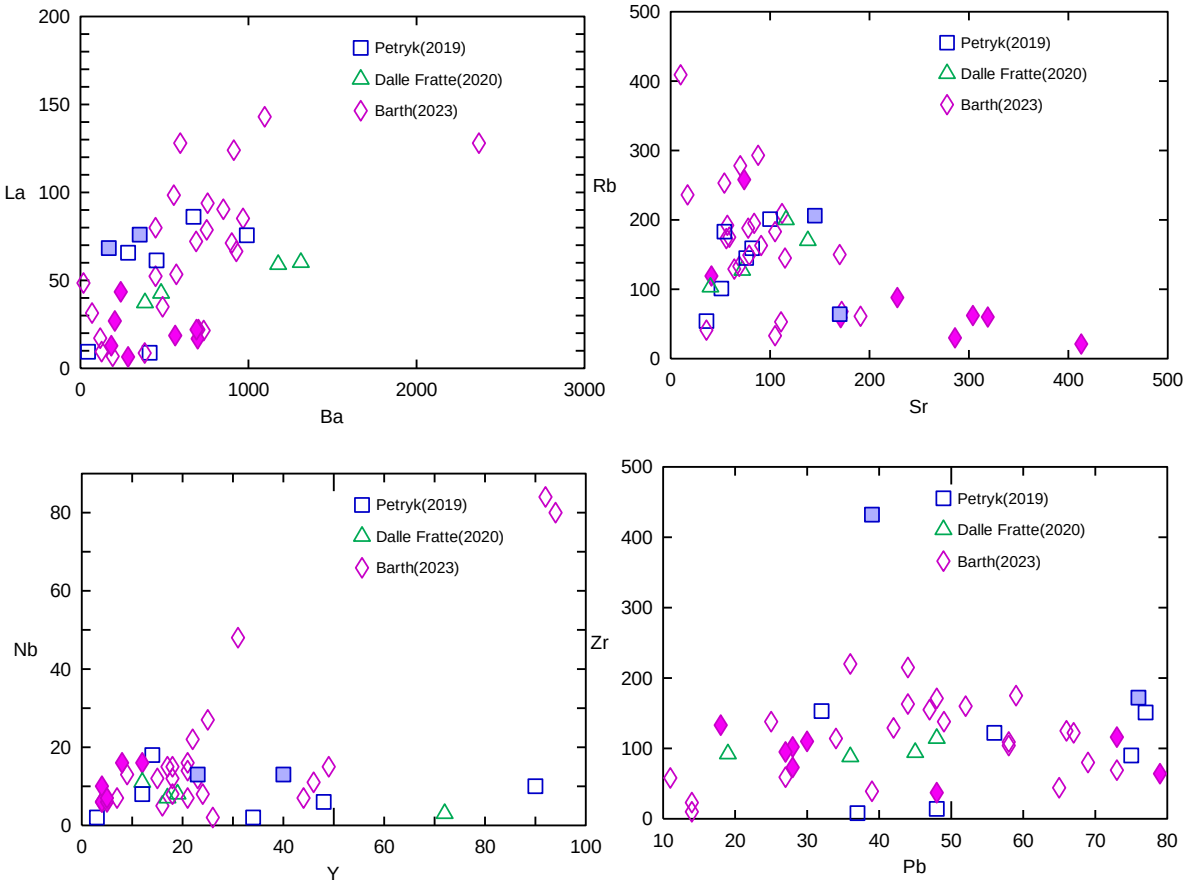

Figure 9. (top left) Barium (ppm) is an incompatible trace cation and Lanthanum (ppm) is the most incompatible R.E.E. Barium Lanthanum ratios can indicate areas where more sediment was recycled. MQ-134 is relatively high in barium. **(top right)** Strontium (ppm) is incompatible in hydrothermal conditions whereas Rubidium (ppm) is compatible. Samples high in strontium are more representative of the host composition of the melt. Which include samples: MQ-130a, MQ-132c, MQ-132d, MQ-135c, and MQ-136. **(bottom left)** High Nb/ Y ratios can indicate melt related enrichment. Two outliers high in both Nb(ppm) and Y(ppm) are most likely the Humboldt Granite. **(bottom right)** Similar trends with all data sets with zircon levels being under 200 ppm, with the exception of BCG-12b from Petryk (2019).

5 Discussion

5.1 Bell Creek batholith petrogenesis

5.1.1 Zircon U-Pb dates

Previous interpretations divided the Southern Complex into two different units based on the age and textures of the rock. The ages of the unit vary but the deformed migmatitic and gneissic rocks were interpreted to be much older than the nondeformed granitoids based on initial mapping (Cannon and Schultz, 1973). The mapped units were considered to be a part of the Northern Complex (named the 'Campeau Creek gneiss or migmatite'), which is upwards of 3.2 Ga; nearly 600 Ma. older than the first dates obtained for the Southern Complex Bell Creek granitoids by Tinkham (1997). Table 2 shows a comparison between the dates obtained by Petryk (2019) and those from this study (Appendix 7). The ages of the different types of granitoids distinguished by texture (i.e. 'normal' and 'clotted') and those of the gneissic and/or migmatitic units are either within error of one another or approximately 50 Ma. The ages calculated from this data support Petryk's interpretation that the Southern Complex is ~2.6 Ga, rather than consisting of two units with distinctly different crystallization ages.

Table 2. Weighted mean age by rock type for the granitoids and gneiss/migmatite. Data from this study in black text; data from Petryk (2019) in blue text.

ROCK TYPE	SAMPLE	CRYSTALLIZATION AGE (MA)	MEAN CRYSTALLIZATION AGE (MA)
BELL CREEK GRANITOID	MQ-116A, MQ-120, MQ-125, MQ-126B, MQ-130A, MQ-144 BCG-1A, BCG-7A, BCG-8A, BCG-4A, BCG-8B, CLG-14B	2607.10±9.64, 2630.19±5.02, 2640.49±7.37, 2632.85±7.96, 2624.20±7.99 2621.05±9.08 2578±56, 2573±37, 2552±17, 2514±21, 2537±40, 2416±42	2,626 2,528
BELL CREEK GNIESS/ MIGMATITE	MQ-118, MQ-130C, MQ-160, MQ-109A BCG-7C	2599.88±3.30, 2694.37±9.48, 2492.60±17.7, 2633.60±24.10 2611±47	2605 2611
HUMBOLT GRANITOID	MQ-122	1538.30±16.40	1538

Clotted granitoids were first defined as a separate unit by Hoffman (1987), but no absolute age was determined, however, based on a cross-cutting relationship a relative age indicating the clotted granitoids were younger than the Bell Creek 'normal' granitoids'. The crystallization age of the clotted granitoids found by Petryk (2019) and in this study though, indicate that there is no resolvable age difference between these two rock types (i.e. all within error).

Dalle Fratte (2020) showed that the migmatitic rocks likely represent a deformed product of mixing between intruding mafic magmas into the felsic Bell Creek granitoid.

Therefore, given the current, large dataset of zircon U-Pb ages presented here that now cover the majority of the study areas from previous work and analyses of the textural relationship between mafic and felsic rocks in the deformed units, it appears that all of these units are a part of one geologic event that may have spanned tens, or even a hundred million years.

5.1.2 Inherited Grains

Inherited ages can be differentiated from the crystallization ages because they are older than the mean age, appearing as outliers within the distribution overall age (Figure 10). Using the Jenks Natural Breaks in the histogram, inherited (red) and metamorphic (blue) grains were selected. Inherited and metamorphic grains from all 11 samples are shown in Table 3. One notable difference between the inherited zircons dated from this study and the Petryk (2019) study is that there were very few dates over 3000 Ma. This could be due to discordance in those grains dated in this study (i.e. unacceptable error in measurement), or generally older basement rock and/or amount of assimilation in the western portion of the Bell Creek batholith compared to the eastern portion.

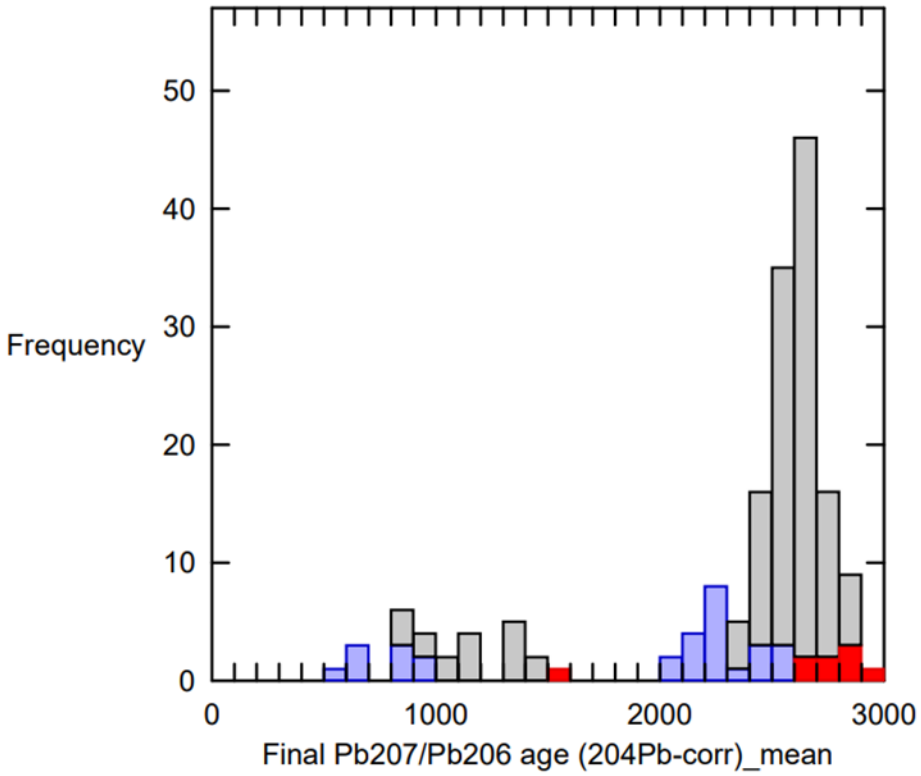

Figure 10. Histogram of the $^{207}Pb/^{206}Pb$ mean age corrected for background lead. Values are shown in (Ma), with a majority between 2500 and 2700. The red inherited grain near 1500 Ma is an inherited grain for the Humboldt Granitoid.

Table 3: Mean age, inherited age, and metamorphic ages of Bell Creek area rocks in Ma.

Sample	U-Pb Mean Age	Inherited	Metamorphic
MQ-116A	2587±13	2743	x
MQ-118	2602.1±4.6	2641	2520, 2518, 2547
MQ-120	2620.5±5.5	2719	x
MQ-122	1349±13	x	586
MQ-125	2587.0±8.8	x	620
MQ-126B	2634.9±7.2	x	2494, 2237
MQ-130A	2548.0±6.9	x	2275, 2216, 2053, 2264
MQ-130C	2819.1±5.9	x	958, 815
MQ-160	2748.7±6.9	2803	x
MQ-109A	2458±22	x	x
MQ-144	2548.5±6.7	x	916, 847, 861, 668

Inherited ages from Table 3 along with the inherited ages from Petryk (2019) are mapped in Figure 11. The inherited grains were divided into three natural breaks using Jenks Natural Breaks. This is a statistical method that clusters data with similar values to reduce the average deviation from the class mean and determines breaks where there are relatively large differences in values. The number of natural breaks was determined by looking at the data distribution in a histogram and with ages ranging from 2600 Ma to 4100 Ma.

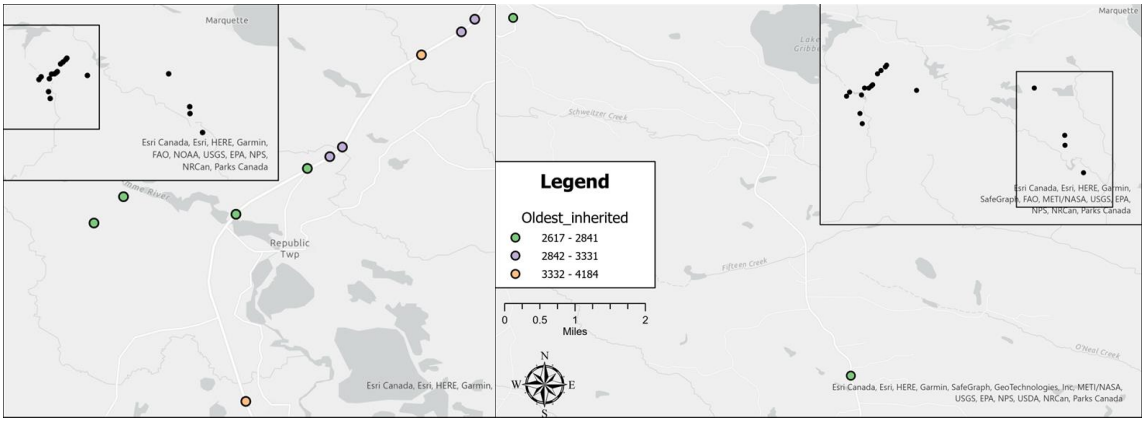

Figure 11. Location of inherited zircon grains found along M-95 and M-35. Inlays indicate where samples were taken along the highways. Since not all sample have inherited grains there are fewer location of inherited grains than overall samples shown on the inlay. Inherited grains were divided into three natural breaks. Both of the inherited grains found along M-35 are younger than 3000 Ma whereas those along M-95 yielded older inherited grains.

In this study, no inherited grains older than 2800 Ma were obtained along the eastern side of the Bell Creek batholith. In contrast, those found along the western side have numerous inherited grains over 3000 Ma. This could indicate that M-35 either had less old material or the older material wasn't preserved as well as the western side of the Southern Complex.

Tinkham (1997) based his interpretation on only two available ages for the Bell Creek Gneiss. His younger date of 2703 Ma is close to the average crystallization age of 2600 Ma for the Bell Creek granitoids and gneiss from this study and Petryk (2019). Alternatively, the older grain with an age of 3093 Ma may have been an inherited, remnant zircon assimilated from the basement rocks. Therefore, based on the new, much more extensive dataset compiled here we interpret the dates obtained by Tinkham (1997) to most likely represent zircon grains that were inherited, rather than representative of the crystallization age of the batholith and/or Northern Complex, Campeau Creek gneiss/migmatites.

5.2 Geochemistry

Major element data from this study expand the spatial extent of sampling from the Bell Creek batholith relative to previous studies (Dalle Fratte; 2020, Hoffman, 1987; Petryk, 2019; Tinkham, 1997) Most of the major element geochemistry from this and other studies is similar among the different areas. However, there is a conspicuous difference in a subset of the data that shows higher Na_2O and CaO, and lower K_2O (filled in symbols) compared to most of the rocks examined by Petryk (2019) – with the exception of two - on the western side (Figure 6) These rocks fall into the category of TTGs (tonalite, tronhjemite, granodiorite) based on having a Na_2O/K_2O ratio greater than 1.5 and are characteristic of magmas produced in the Archean.

The new trace element data also distinguishes these TTG rocks from the others in having a high Sr/Y ratio (Figure 12). This ratio is used as a proxy for depth of magma production. In crustal level magmas, shallow genesis favors the production of

plagioclase, whereas deep genesis favors the production of garnet (great than ~35km). Strontium is a highly compatible element in plagioclase and yttrium is highly compatible in garnet. Therefore, rocks that have a high Sr/Y ratio are produced at depths greater than ~35km in the crust. All of the TTG samples from this study appear to be produced at high pressures, whereas the two TTG samples from the Petryk (2019) study were produced at low pressures.

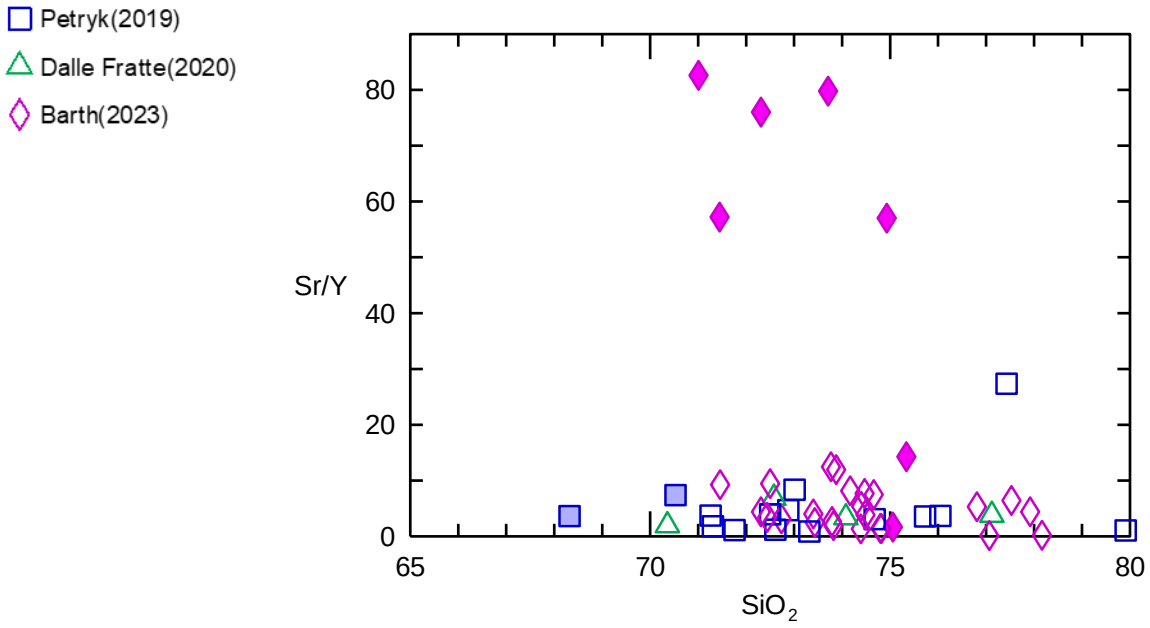

Figure 12. Sr/Y ratio plotted against SiO_2. Filled symbols represent higher Na_2O and CaO, and lower K_2O.

5.3 Tectonic setting and crustal assimilation

In general, major and trace-element data from this region indicate that Bell Creek granitoids formed in a volcanic arc setting (Figures 13 and 14). A few samples plot outside of the volcanic arc and I-type region and into the within-plate and A-type granitoid (Figure 13) region. Data from this study that are firmly within those regions are

part of the younger (~1350 Ma), alkaline Humbolt granite, which would have been injected into the existing Bell Creek batholith. Therefore, both the age and geochemistry are consistent with the Bell Creek batholith having been constructed within a continental arc setting during the Neoarchean Era.

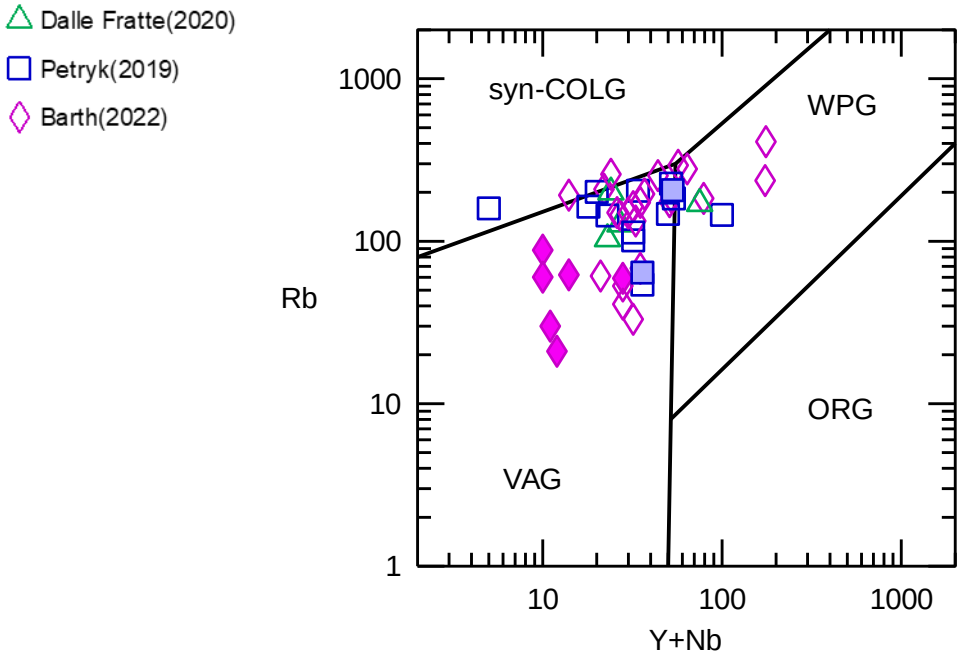

Figure 13. Granitoid discrimination diagram from Pearce et al (1984).

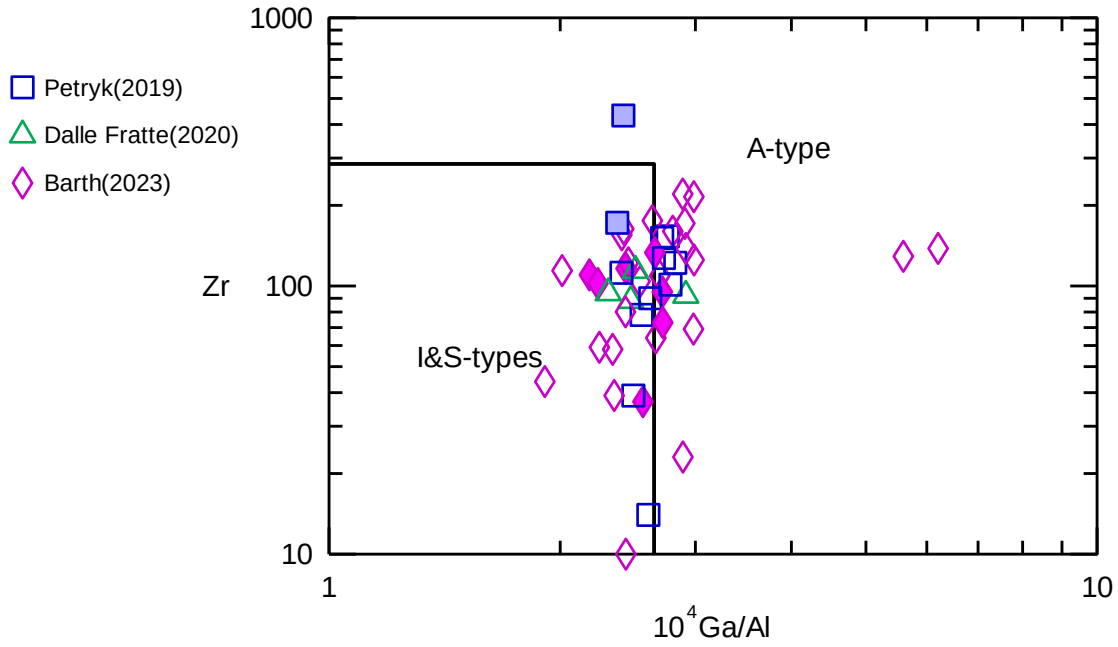

Figure 14. Discrimination diagram for granitoids (Whalen et al., 1987).

Hoffman (1987) first determined that the Bell Creek granitoid is an S-type and suggested that it was derived from melting of amphibolite in the deeper crust with assimilation of a pelitic source material - possibly a graywacke, shale, or arkose. Indeed, the Shand's Index does show the slightly peraluminous character of these rocks (Figure 15), which likely reflects the addition/contribution from one or more of the abovementioned sedimentary or metasedimentary sources. The Bell Creek granitoid is also enriched in LIL/HFS (Figure 7) and has elevated Na_2O+K_2O (Figure 6), which reflects input from a crustal source.

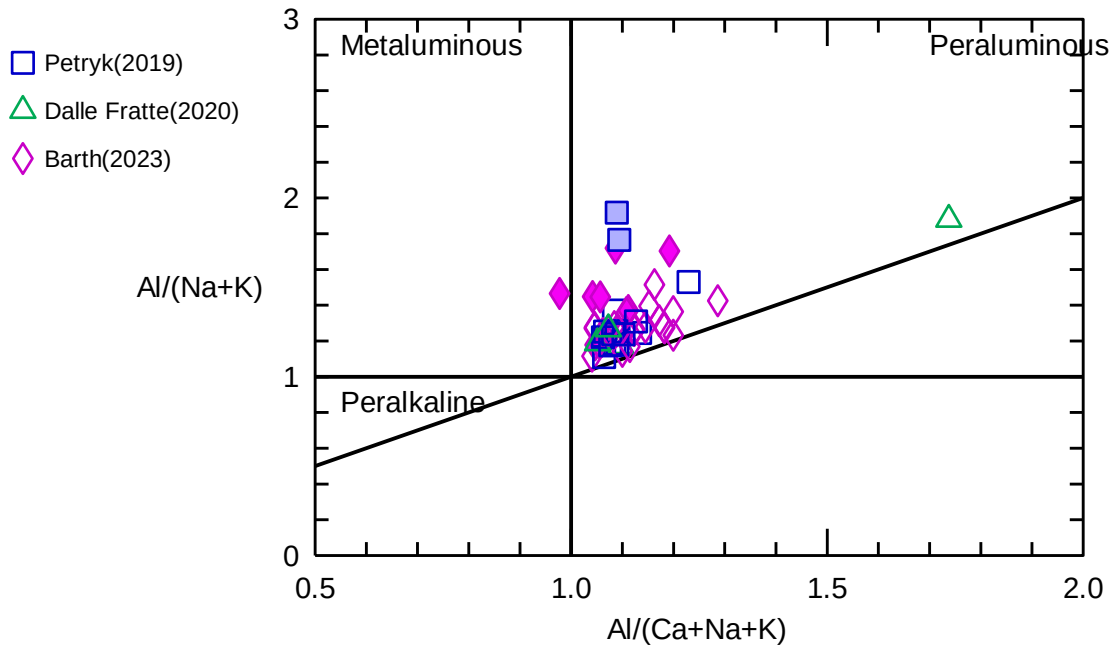

Figure 15. Shand's Index (Maniar and Piccoli, 1989) showing the slightly peraluminous character of the Bell Creek units. An outlier from Dalle Fratte (2020) is highly peraluminous, but this is likely due to alteration.

Petryk (2019) was the first to conduct a study of the oxygen isotopic composition of zircons from the Bell Creek granitoids to determine the crust-mantle contributions in the petrogenetic evolution. It was found that most of the zircons in the granitoids had mantle-like $\delta^{18}O$ values (~5.5‰), but there were higher values (up to ~12‰) indicating that some crustal assimilation occurred consistent with other geochemical evidence presented here and in previous studies. Importantly, the evidence presented in these studies, including this one, indicate that, during the late Archean, crustal level crystal fractionation with some amount of assimilation was the dominant process that formed the batholith. Therefore, we conclude that a net addition of new crust occurred during this period at a continental arc setting.

5.3.1 Regional Context

In the Superior Province there was possibly a stagnant lid episode in volcanism which occurred between ~2.9-2.8 Ga (Wyman,2018). Around 2.7 Ga there were widespread shallow mantle plumes in the transitional zone (Wyman, 2015), as shown in Figure 16. This figure shows that during the final phase of subduction at the Wawa Arc (D) felsic magmatism began to dominate, which would have formed the Southern Complex.

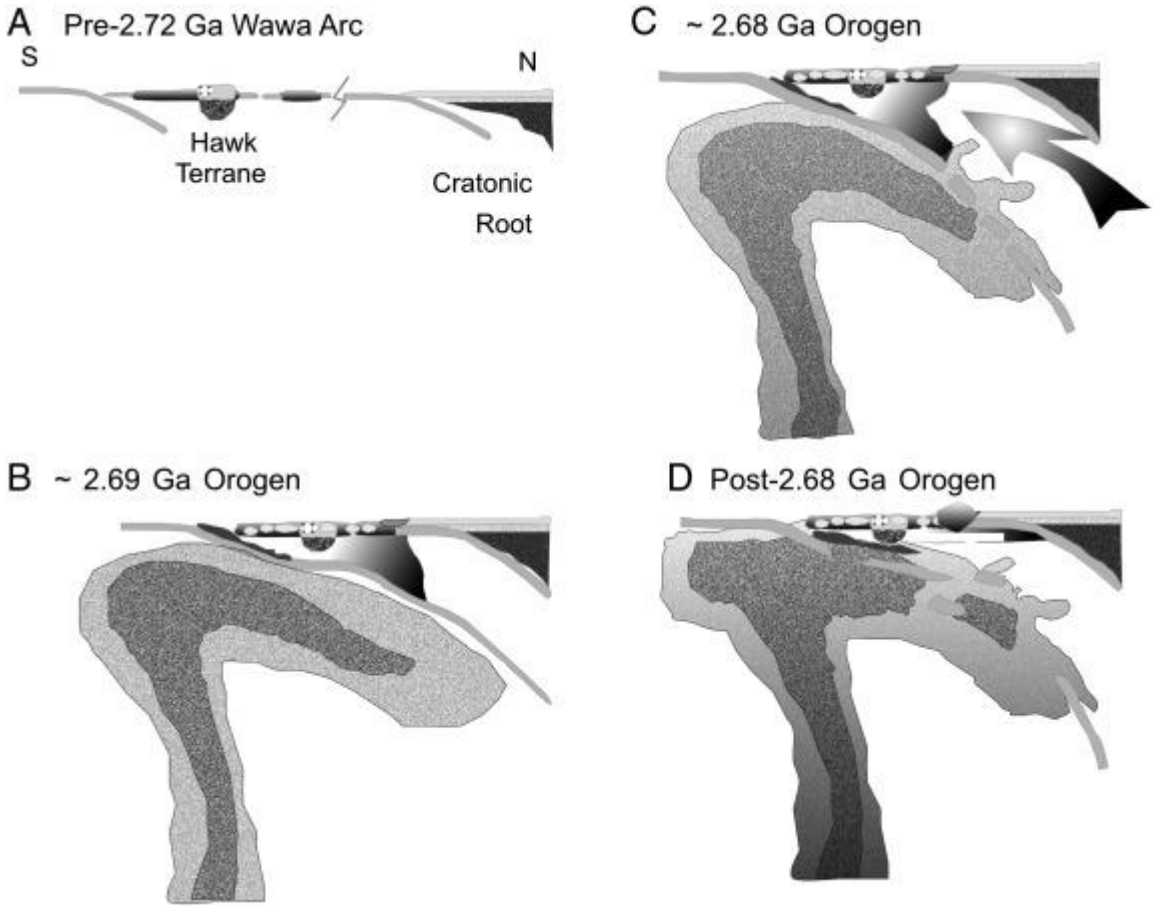

Figure 16. Figure from Wyman, (2015). In figure D of the subduction of the Wawa arc is when a felsic complex would begin to form, such as the Southern Complex.

6 Conclusion

The results of this study indicate that the composition and ages of the eastern side of the Bell Creek batholith are very similar to those of the western side of the Bell Creek batholith previously investigated by Dalle Fratte (2020), Hoffman (1987), Petryk (2019), and Tinkham (1997). The eastern side of the batholith also exhibits slight variations in geochemistry, which supports Dalle Fratte's (2020) interpretation of the Southern Complex forming during magma mixing between a felsic melt and several generations of a more mafic melt intruding the pluton during or later in its crystallization. It would be valuable to investigate oxygen-hafnium isotopes from the eastern part of the Southern Complex and compare this to the results from Petryk (2020), This would help to determine the extent of assimilation across the batholith and, therefore, the amount of additional continental crust produced during this time period.

7 Bibliography

Barth, T. F. W. (1952). *Theoretical Petrology: A Textbook on the Origin and the Evolution of Rocks.* New York: Wiley; London: Chapman & Hall.

Cannon, W. F., & Simmons, G. C. (1973). Geology of Part of the Southern Complex, Marquette District. *Michigan: Journal of Research of the U.S. Geological Survey*, *1*(2), 165-172. https://doi.org/70160638

Card, K. D., & Ciesielski, A. (1986). DNAG #1. Subdivisions of the Superior Province of the Canadian Shield. Geoscience Canada, 13(1). Retrieved from https://journals.lib.unb.ca/index.php/GC/article/view/3439

Dalle Fratte, A., Deering, C. D., DeGraff, J. M., & Malaspina, N. (2020). Geochemical and Petrological Evidence of the Geodynamic Evolution of the Bell Creek Batholith, Republic Quadrangle, Marquette. Michigan Technological University.

Hammond, R. D. (1978). *Geochronology and origin of Archean rocks in Marquette County, Upper Michigan* (thesis). University of Kansas M.S. thesis, Lawrence, Kans.

Hoffman, M. (1987). The southern complex : geology, geochemistry, mineralogy and mineral chemistry of selected uranium- and thorium-rich granites. Thesis (Ph.D.)--Michigan Technological University, 1987.

Home. Zirchron. (n.d.). Retrieved March 25, 2023, from https://www.zirchron.com/

Kay, R. W. (1984). Elemental abundances relevant to identification of magma sources. *Philosophical Transactions of the Royal Society of London. Series A, Mathematical and Physical Sciences*, *310*(1514), 535–547. https://doi.org/10.1098/rsta.1984.0007

Krauskopf, K. B. (1967). *Introduction to geochemistry: International studient edition*. Mcgraw-Hill, Tokyo.

Paton, C., Hellstrom, J., Paul, B., Woodhead, J., & Hergt, J. (2011). Iolite: Freeware for the visualisation and processing of mass Spectrometric Data. *Journal of Analytical Atomic Spectrometry*, *26*(12), 2508. https://doi.org/10.1039/c1ja10172b

Paton, C., Woodhead, J. D., Hellstrom, J. C., Hergt, J. M., Greig, A., & Maas, R. (2010). Improved laser ablation U-Pb zircon geochronology through robust downhole fractionation correction. *Geochemistry, Geophysics, Geosystems*, *11*(3). https://doi.org/10.1029/2009gc002618

Petrus, J. A., & Kamber, B. S. (2012). Vizualage: A novel approach to laser ablation ICP-MS U-PB geochronology data reduction. *Geostandards and Geoanalytical Research, 36*(3), 247–270. https://doi.org/10.1111/j.1751-908x.2012.00158.x

Petryk, Deering, C., Bornhorst, T., & Bachmann, O. (2019). The Origin of an Archean Batholith in Michigan's Upper Peninsula. Michigan Technological University.

Schmus, W. R., & Woolsey, L. L. (1975). Rb–Sr geochronology of the Republic area, Marquette County, Michigan. *Canadian Journal of Earth Sciences, 12*(10), 1723–1733. https://doi.org/10.1139/e75-153

Schulz, K. J., & Cannon, W. F. (2007). The Penokean orogeny in the Lake Superior region. *Precambrian Research, 157*(1-4), 4–25. https://doi.org/10.1016/j.precamres.2007.02.022

Tinkham, D. K., & Marshak, S. (1997). *Tectonic evolution of the southern complex region of the Penokean Orogenic Belt, Upper Peninsula, Michigan: The formation of Precambrian Dome-and-keel architecture* (thesis).

Vermeesch, P. (2018). ISOPLOTR: A free and open toolbox for geochronology. *Geoscience Frontiers, 9*(5), 1479–1493. https://doi.org/10.1016/j.gsf.2018.04.001

Wyman, Hollins, P. (2018). Do cratons preserve evidence of stagnant lid tectonics? Di Xue Qian Yuan., 9(1), 3–17. https://doi.org/10.1016/j.gsf.2017.02.001

Wyman, Hollings, P., & Conceição, R. V. (2015). Geochemistry and radiogenic isotope characteristics of xenoliths in Archean diamondiferous lamprophyres: Implications for the Superior Province cratonic keel. Lithos, 233, 111–130. https://doi.org/10.1016/j.lithos.2015.02.018

.

A Copyright Documentation

Figure 1: from Cannon and Simmons, 1973

Figure 2: Tinkham (1997) modified from Hoffman (1987).

Figure 16: Wyman (2015)